

# Theory of high-density optical effects on polaritons in $\text{Cu}_2\text{O}$ : Bistability and optical hysteresis

Oleksiy Roslyak and Joseph L. Birman

*Physics Department, The City College, CUNY, Convent Avenue at 138 Street, New York, New York 10031, USA*

(Received 9 February 2007; revised manuscript received 24 October 2007; published 25 February 2008)

We present a comparative analysis of a “conventional” phonoriton (coherent superposition of exciton-photon-phonon) versus a polariton (coherent exciton-photon superposition) which is “weakly” coupled to the longitudinal acoustic-phonons bath. Depending on the duration of the pumping laser field, the phonon-induced decoherence results in two distinct types of excitation. Long (millisecond) laser pumping pulses form an “equilibrium” polariton. The generic feature here is a pronounced photothermal bistability, i.e., formation of four distinct branches. Transitions between branches can be achieved by excitation energy fluctuations as small as 200 neV. This may impede Bose-Einstein condensation of the para-excitons. Short (microsecond) laser pulses create a “quasiequilibrium” polariton. In the latter case, for some critical intensity of the laser field, we demonstrate the possibility of strong luminescence from a highly unstable localized state on the lower polariton branch.

DOI: [10.1103/PhysRevB.77.075206](https://doi.org/10.1103/PhysRevB.77.075206)

PACS number(s): 71.35.Gg, 71.35.Lk, 71.36.+c

## I. INTRODUCTION

Cuprous oxide is considered as a probable candidate for Bose-Einstein condensation (BEC) of excitons.<sup>1-4</sup> The extremely small mass of the excitons allows them to condense at temperatures much higher than those of such atomic systems as helium or alkali metals.<sup>5</sup> The lowest excited states of cuprous oxide are classified following the cubic symmetry of the lattice ( $O_h$ ). This gives the nondegenerate ortho-exciton (OE) ( $\Gamma_5^+$ , binding energy  $E_b=150$  meV) and triple-degenerate para-exciton (PE) ( $\Gamma_2^+$ ,  $E_b=162$  meV). Due to its even parity, OEs are quadrupole active, and PEs remain optically inactive in one photon absorption experiments. However, the PE can be effectively populated from the OE by emitting optical phonons or in two photon experiments. For samples of high purity (more than 99.99%), the linewidth of the OE is very narrow ( $\Gamma_{15} \approx 0.8$   $\mu\text{eV}$  for  $T=2$  K) and determined mostly by the OE to PE conversion rate. This narrowness is responsible for the extremely long lifetime and expected (nanosecond) BEC coherence time for the PE.<sup>6</sup>

There are two main nonstatistical mechanisms impeding expected BEC in bulk cuprous oxide samples. First is two-exciton nonradiative Auger heating.<sup>7</sup> It was shown that the OEs move along the phase boundary without crossing it,<sup>8</sup> as a consequence of the balance of entropy changes due to cooling of excitons by phonons and heating by the nonradiative Auger two-exciton recombination process. The Auger annihilation rate for para-para collisions is much smaller than that for OE-PE and OE-OE collisions, explaining why the PEs are likely to condense while the OEs fail to do so. A second impeding mechanism is the relatively strong light-matter interaction producing polaritons which tend to escape the crystal before condensation occurs.<sup>3</sup> For the polaritons to experience BEC, there is a criterion of smallness imposed on the exciton-photon coupling. Only the PEs meet the criteria,<sup>2</sup> but as far as we know, there is no conclusive evidence of BEC in the bulk cuprous oxide.

In this paper, we examine another possible mechanism obstructing BEC. Namely, a weak coupling of the polariton branches with long wavelength acoustic phonons and the ef-

fective formation of a phonon-perturbed polariton. For low pumping intensity and in close proximity to the exciton-photon resonance, one can consider “weak” coupling to the longitudinal acoustic (LA) phonons<sup>9</sup> and treat the phonons semiclassically by means of some effective temperature dependence of the exciton energy. Namely, in the case of weak (but not negligible) electron-phonon coupling, the semiconductor gap energy (and, thus, the energy of the exciton) decreases. There is experimental evidence of the exciton energy redshift for various semiconductors<sup>10</sup> as well as for  $\text{Cu}_2\text{O}$  at helium temperatures.<sup>11</sup>

In Sec. II, we compare this weakly perturbed polariton versus the concept of conventional phonoriton as an excitation formed by resonance interaction between the exciton, photon, and phonon.<sup>12</sup> The resulting polariton branches strongly depend on what kind of heating and cooling mechanisms dominate.

In Sec. III, we investigate the pumping of a cuprous oxide thin film by short laser pulses (microsecond). In this regime, the heating is a result of “phonon-assisted” Auger process<sup>7</sup> and the cooling is provided by LA phonons. The polaritons come to quasiequilibrium and, due to the temperature dependence of the exciton energy, the dispersion is modified. Consequently, we show that localized states exist on the lower branch of this polariton.

In Sec. IV, we regard long laser pulses (millisecond). In this case, the temperature is defined by the laser heating and temperature exchange with the surrounding helium. We demonstrate that this results in temperature bistability and splitting of the dispersion curves into four distinct branches.

Numerical estimates of the decoherence effects are performed in Sec. V using realistic cuprous oxide material parameters. According to our calculations, this splitting and phonon-induced decoherence may effectively obstruct BEC of the PE in cuprous oxide.

## II. POLARITON WEAKLY PERTURBED BY LONGITUDINAL ACOUSTIC PHONONS VERSUS CONVENTIONAL PHONORITON

Let us consider a thin film of cuprous oxide ( $d_s=30$   $\mu\text{m}$ ) placed in a helium bath at temperature  $T_{\text{bath}}$

=1.7 K and pumped by laser pulses of varying power  $P_{ex}$ . The pumping laser field is polarized along  $(1\bar{1}0)$  and has the wave vector  $\mathbf{k}$  parallel to the  $(111)$  direction. The laser is tuned into resonance with dipole forbidden, quadrupole allowed  $1S$  exciton ( $\hbar\omega_{1S,0}=2.05$  eV for OE and  $\hbar\omega_{1S,0}=2.05-0.097$  eV for PE). The exciton mass and radius are  $M=3m_0$  and  $a_B\approx 5.1$  Å, respectively. From the selection rules, it follows that only the OEs ( $1/\sqrt{2}$ ) ( $\Gamma_{5x}^+-\Gamma_{5y}^+$ ) are optically allowed with the oscillator strength of the transition  $f_{o,[111]}=3.7\times 10^{-9}$ . The PEs acquire some oscillator strength  $f_p=4f_o10^{-3}$  in a magnetic field or under an external stress through spin-orbit interaction.

The conventional phonoriton<sup>12-15</sup> is a quasilinear mode depending parametrically on the intensity of the pump light ( $P_{ex}$ ), and characterizes a coherent superposition of exciton, photon, and phonon when the up-conversion process is allowed. The laser pulse induces a pump polariton with the exciton wave vector  $\mathbf{p}$  and energy  $\hbar\omega_p$ . The excitonic component of the polariton couples with other excitonic modes  $\mathbf{k}$  due to the exciton-LA-phonon interaction. To form a conventional ‘‘phonoriton,’’ the laser intensity should be big enough to have the exciton-LA-phonon coupling:

$$Q_{\mathbf{k}-\mathbf{p}} = D_{ex} \sqrt{\frac{n_o |\mathbf{p}-\mathbf{k}|}{2\hbar\rho v_{ph}}} \sim \sqrt{\frac{P_{ex}}{v_g}} \quad (1)$$

comparable with the exciton-photon interaction  $\Omega_{rabi} = \sqrt{f_o} E_{1S} \approx 124$   $\mu\text{eV}$ . Here, we introduced  $D_{ex}$  as the exciton deformation potential,  $\rho$  is the mass density, and  $v_g$  and  $n_o$  are the group velocity and density, respectively, of the polariton. In terms of creation (annihilation) operators, the exciton ( $b_{\mathbf{k}}^\dagger$ )-photon ( $c_{\mathbf{k}-\mathbf{p}}^\dagger$ )-phonon ( $\alpha_{\mathbf{k}}^\dagger$ ) Hamiltonian of the cuprous oxide crystal has the form

$$\begin{aligned} \frac{H}{\hbar} = & (\omega_{1S,\mathbf{k}} - \omega_p) b_{\mathbf{k}}^\dagger b_{\mathbf{k}} + (\omega_{\mathbf{k}}^{photon} - \omega_p) \alpha_{\mathbf{k}}^\dagger \alpha_{\mathbf{k}} + \Omega_{\mathbf{p}-\mathbf{k}}^{phonon} c_{\mathbf{k}-\mathbf{p}}^\dagger c_{\mathbf{k}-\mathbf{p}} \\ & + \frac{i}{2} \Omega_{rabi,\mathbf{k}} (\alpha_{\mathbf{k}}^\dagger b_{\mathbf{k}} - b_{\mathbf{k}}^\dagger \alpha_{\mathbf{k}}) + Q_{\mathbf{k}-\mathbf{p}} (b_{\mathbf{k}}^\dagger c_{\mathbf{k}-\mathbf{p}} - c_{\mathbf{k}-\mathbf{p}}^\dagger b_{\mathbf{k}}). \end{aligned}$$

Here,  $\omega_{\mathbf{k}}^{photon} = ck/\sqrt{\epsilon_\infty}$  and  $\Omega_{\mathbf{p}-\mathbf{k}}^{phonon} = v_s |\mathbf{k}-\mathbf{p}| \approx 155$   $\mu\text{eV}$  are the photon and phonon dispersions at the exciton-photon resonance  $k_0 = 2.62 \times 10^5$   $\text{cm}^{-1}$ ;  $\epsilon_\infty = 6.5$  is the background dielectric constant; and  $v_s$  is the LA-sound velocity. The eigenvalues of the Hamiltonian above are given by an implicit phonoriton dispersion:

$$\begin{aligned} & (\omega_{1S,\mathbf{k}} - \omega) (\omega_{\mathbf{k}}^{photon} - \omega) (\omega_p + \Omega_{\mathbf{k}-\mathbf{p}}^{phonon} - \omega) \\ & - Q_{\mathbf{k}-\mathbf{p}}^2 (\omega_{\mathbf{k}}^{photon} - \omega) - \frac{\Omega_{rabi,\mathbf{k}}^2}{4} (\omega_p + \Omega_{\mathbf{k}-\mathbf{p}}^{phonon} - \omega) = 0. \end{aligned} \quad (2)$$

In contrast to the standard picture of phonon-mediated polariton scattering, the dispersion is strongly modified from the polariton dispersion and consists of three dispersion branches. Around the exciton-photon resonance, such coherent polariton-phonon interaction results in an effective ‘‘blue-shift’’ of the ‘‘polaritonlike’’ branch of the phonoriton.

The key point in the phonoriton picture is the coherence between all the particles involved. However, for small density of polaritons, the polariton-phonon interaction (1) is weak. We define the weak polariton-phonon coupling as a limiting case of conventional phonoriton when the down-conversion<sup>16</sup> processes are dominant and up-conversion<sup>17</sup> processes are negligible. Therefore, in close proximity to exciton-photon resonance, this weak interaction with the LA-phonons bath manifests itself by the small decoherence between exciton and photon in the polariton.

We propose to treat the LA phonons semiclassically and use the deviation of the polariton gas temperature from the temperature of the helium bath  $T - T_{bath}$  as that small decoherence parameter. To estimate the influence of the temperature deviation on the polariton dispersion, we adopt the following picture of the exciton-phonon interaction.

The electron and hole of the exciton part of the polariton move in the cloud of LA phonons (we neglect TA phonons, as their contribution to the interaction is much weaker at the given temperature range<sup>7</sup>). The result is a bigger mass of the exciton and redshift of the *energy gap* between the conduction and valence bands without a noticeable effect on the binding energy of the  $1S$  exciton.<sup>6</sup> There is experimental evidence for such exciton-phonon interaction. Exciton energy ‘‘redshift’’ has been observed for several types of semiconductor<sup>10</sup> and specifically for  $\text{Cu}_2\text{O}$  at helium temperatures.<sup>11</sup>

According to the general formulation of the theory,<sup>18</sup> this temperature dependence is accurately given by integrals of the form

$$\begin{aligned} \omega_{1S,0}(T) - \omega_{1S,0}(T_{bath}) = & -\frac{1}{2} \int d\omega f(\omega) \\ & \times \left[ \coth\left(\frac{\hbar\omega}{2k_B(T - T_{bath})}\right) - 1 \right]. \end{aligned} \quad (3)$$

Here,  $\coth\left(\frac{\hbar\omega}{2k_B(T - T_{bath})}\right) - 1$  represents the average phonon occupancy number and  $f(\omega)$  is the relevant electron-phonon spectral function.

Expanding Eq. (3) into a series around the bath temperature, in the linear approximation the dispersion of this perturbed polariton is given by the following system of equations:

$$\begin{aligned} & [\omega_{1S,\mathbf{k}}(T) - \omega] (\omega_{\mathbf{k}}^{photon} - \omega) - \frac{\Omega_{rabi,\mathbf{k}}^2}{4} = 0, \\ \hbar\omega_{1S,\mathbf{k}}(T) = & \hbar\omega_{1S,0}(T_{bath}) + \frac{\epsilon_\infty \hbar^2 k^2}{2M} + \kappa(T - T_{bath}). \end{aligned} \quad (4)$$

In the last expression, the parameter  $\kappa = 0.30$   $\mu\text{eV K}^{-1}$  is experimentally determined.<sup>11</sup> The resulting polariton branches are given by the equations above along with a temperature equation which is strongly dependent on what kind of heating and cooling mechanisms prevail (see Fig. 1). Therefore, in the next sections, we are going to consider two distinct cases:

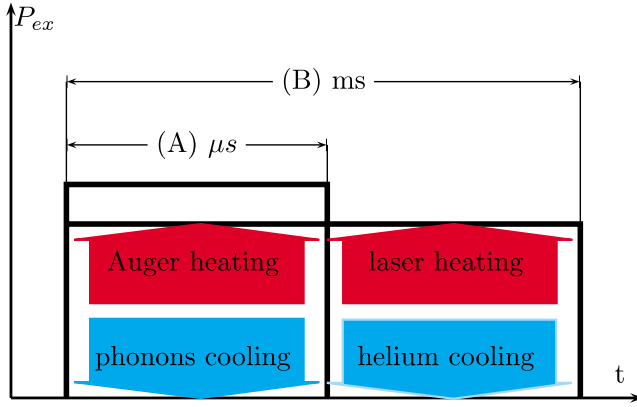


FIG. 1. (Color online) Schematic of different heating (cooling) mechanisms in the thin film of cuprous oxide. Different mechanisms create different thermal regimes of the sample and result in different polariton dispersions. Case (A) corresponds to short excitation pulses, with  $T$  the temperature of the exciton gas and  $T_{bath}$  the temperature of the LA phonons; and case (B) corresponds to long pulses, with  $T$  the temperature of the LA phonons and  $T_{bath}$  the temperature of the surrounding helium.

(A) Short (microsecond) laser pulses, where heating is a result of phonon-assisted Auger process<sup>7</sup> and the cooling is caused by LA phonons. In picosecond dynamics, the system comes to quasiequilibrium and, due to the temperature dependence of the excitonic part of the polariton, there is a distinct change in the dispersion.

(B) Long (millisecond) laser pulses are applied, which leads to the temperature being defined by photothermal laser heating and temperature exchange with the surrounding helium. This will result in a photothermal bistability effect.

Note that the polaritonlike branches of the phonoriton given by Eq. (2) can be formally obtained from the system of equations (4) by modeling the up-conversion processes with the additional condition  $T_{bath} > T$ . However, the physical meaning of the system of equations (4) is rather different. In our treatment, the phonons are not mediators for the exciton-exciton interaction, but the source of decoherence for the pump polariton.

### III. SHORT LASER PULSES

First, we consider short laser excitation [see Fig. 1(a)]. Therefore, the system of interacting  $1S$  quadrupole excitons, photons, and low energy LA phonons can be treated adiabatically.

In the equation governing the dynamics of the temperature, we neglect all ultrafast processes (pico- and nanosecond dynamical processes), such as optical phonon cooling (characteristic time  $\tau = 0.2 \times T^{-1/2}$  ns), radiative decay ( $\approx 300$  ns), and ortho-to-para down-conversion ( $\approx 0.014 \times T^{3/2}$  ns<sup>-1</sup>).<sup>7</sup>

The main sources of heating in this adiabatic system are the nonradiative direct process and phonon-assisted Auger process, with the characteristic Auger decay time  $\approx 0.1 \times T^{-3/2}$   $\mu$ s. Because the conduction and valence bands share the same parity, the rate of direct Auger process is negligibly small. Hence, one has to consider a phonon-

assisted Auger process. This is defined as exciton-exciton recombination into hot electron hole carriers accompanied by emission of a cascade of phonons (see Ref. 7 for more complete discussion).

The rate of change of the entropy of the excitons is a balance between the entropy loss due to phonon cooling and gain due to heating following Auger annihilation of the excitons. The rate of phonon cooling, which is dominated by emission of acoustic phonons, varies as  $-a_1 T^{3/2} (1 - T_{bath}/T)$ . On the other hand, heating of the excitons from the Auger process is proportional to the density of the polaritons  $a_2 n_0$ .<sup>19</sup> The ratio of the coefficients  $a_1/a_2$  varies from  $4.75 \times 10^{22}$  to  $5.71 \times 10^{22}$  and rapidly grows with the increase in duration of the pulses.<sup>7</sup> This emphasizes the fact that for long pulses, one can neglect the effect of the Auger heating compared to phonon cooling. Then, one has to consider direct heating by the laser field. Quantitative comparison of the thermal redshift versus other high density effects reported so far for the cuprous oxide crystals can be found in the Appendix.

Consequently, with increasing temperature, the exciton density grows along the “quasiequilibrium” adiabat:

$$-a_1 T^{3/2} (T - T_{bath}) + a_2 n T = 0,$$

$$n(\omega, T) = \frac{4P_{ext}}{\pi d^2 \hbar \omega_{1S} v_g},$$

$$v_g^{-1} = \frac{\sqrt{\epsilon_\infty}}{c} \frac{\partial x}{\partial \hbar \omega} \approx \frac{\sqrt{\epsilon_\infty}}{c} \frac{x - \hbar \omega}{\hbar \omega_{1S,x}(T) - \hbar \omega}. \quad (5)$$

Here,  $x = \hbar c k / \sqrt{\epsilon_\infty}$  is the energy of the pumping laser field.

The system of equations (5) and (4) has only one solution for the temperature (no bistability). Therefore, it can be numerically solved into the upper and lower branches of the perturbed polariton. To specify the branches for the phonoriton, we put the following conditions for the upper and lower branches, respectively:

$$\lim_{x \rightarrow x_0^+, x \rightarrow x_0^-} \frac{\hbar}{x} \frac{\partial \omega}{\partial x} = 1. \quad (6)$$

In close proximity to the exciton-photon resonance ( $x_0 = \hbar \omega_{1S}$ ) and for small light intensities, the solution of the nonlinear system of equations (5) and (4) can be obtained by perturbation theory. Therefore, in first order, we set an appropriate (6) unperturbed group velocity into the second equation of the system (5) and solve the corresponding algebraic system of equations (4) for the upper and lower branches of the perturbed polariton. The resulting polariton dispersion ( $E = \hbar \omega$ ) as a deviation from the exciton energy ( $E_{1S,x} = \hbar \omega_{1S,k}$ ) is presented in Fig. 2.

For high laser intensities ( $P_{ext} > 25$  mW), the first approximation is not enough, and one must carry on with more iterations,<sup>20</sup> which reduces the redshift effect, as the group velocity grows.

The physics behind different levels of perturbation can be described as follows. In zero approximation, a short laser pulse of energy close to the resonance  $x_0$  enters the system

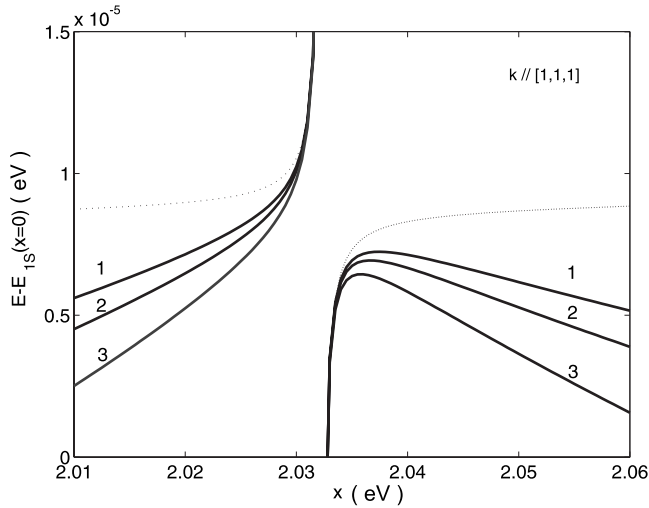


FIG. 2. Polaron dispersion for short pump laser pulse and quasiequilibrium of the exciton gas with the phonon bath. The phonon-assisted Auger process heats the exciton gas, and weak interaction with LA phonons cools it down. Solid lines represent two polariton branches for varying laser intensity: (1)  $P_{ex}=5$  mW, (2)  $P_{ex}=10$  mW, and (3)  $P_{ex}=25$  mW. The dashed line corresponds to the unperturbed polariton:  $P_{ex}<5$  mW.

and creates a polariton wave. The temperature of the system is equal to  $T_{bath}=1.7$  K.

In first approximation, the polariton is relaxed due to polariton-exciton interaction. On the excitonlike part of the polariton (away from  $x_0$ ), this leads to heating due to Auger process and, as a consequence, the redshift of the exciton energy. The perturbed polaritons accumulate on the lower branch according to their new group velocity. The polariton density buildup ( $P_{ex}=5$  mW) is illustrated in Fig. 3.

In the second approximation, this energy change increases the group velocity of the polariton waves and the exciton density is reduced and so is the temperature of the polariton gas. Therefore, the polariton branches swing slightly back to the unperturbed polariton dispersion. Presumably, quasiequilibrium between the Auger heating and LA-phonon cooling is established after some more steps.

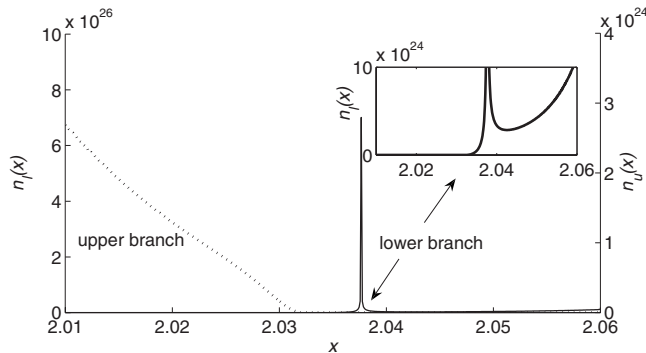


FIG. 3. Density of polariton upper ( $n_u$ ) and lower ( $n_l$ ) branches in first approximation, which must be used for the second approximation in the perturbation. The density peak represents the polaritonic buildup on the lower branch as the result of high localization ( $v_g \rightarrow 0$ ).

#### IV. LONG LASER PULSES

Now let us consider the case of long (millisecond) pumping signals. Contrary to the adiabatic case of short pulses, the heating is due to laser radiation, and cooling is due to surrounding helium [see Fig. 1(b)] for the open system. As we are about to demonstrate, this results in the temperature bistability and splitting of the dispersion curves into four different branches.

The bistability effect is due to the nonlinear origin of the temperature equation.<sup>11</sup> The heating process is proportional to the absorption inside the semiconductor film and, therefore, strongly depends on the polariton dispersion and proximity to the exciton-photon resonance. Neglecting reflection, one can define the absorption through the temperature dependent transmission as  $1-\text{Tr}(T)$ . Therefore, the equilibrium temperature is given by the stationary solution of the following time ( $\tau$ ) dependent system of equations:

$$\frac{dT}{d\tau} = HP_{ex}[1 - \text{Tr}(\hbar\omega, T)] - C[T - T_{bath}],$$

$$\text{Tr}(\hbar\omega, T) = \exp\left[-\frac{\Gamma_{1s}^2}{4[\hbar\omega_{1s}(x, T) - \hbar\omega]^2 + \Gamma_{1s}^2} \frac{d_s}{l_a}\right]. \quad (7)$$

Here, the phenomenologically introduced constants  $H=5.0 \times 10^6$  K s<sup>-1</sup> W<sup>-1</sup> and  $C=2.8 \times 10^3$  s<sup>-1</sup> give the heating and cooling rates, respectively;  $\Gamma_{1s}=0.8$   $\mu$ eV is the phenomenological linewidth and the absorption length is given by

$$l_a = \frac{\Gamma_{1s}\hbar c\sqrt{\epsilon_\infty}}{f_0\hbar\omega_{1s,x_0}^2}.$$

The factor 1/4 counts single-degenerate OE and triple-degenerate PE.

For a qualitative description of the bistability, we fix the wave vector at energy  $x=\hbar\omega=2.01$  eV slightly off the resonant value  $x_0$  and consider only the upper branch of the perturbed polariton. Then the heating part  $HP_{ex}[1-\text{Tr}(\hbar\omega, T)]$  of the temperature equation (7) has a Gaussian shape, with the maximum dependent on detuning from the polariton energy. Depending on the value of the detuning, it can cross the cooling line  $C[T-T_{bath}]$  on the phase diagram ( $\partial T/\partial\tau$  vs  $T$ ) in one, two, or three points on the temperature scale. The last case corresponds to a strong nonlinearity and a hysteresis loop for the temperature in momentum-energy space.

If one moves from higher to lower energy [detuning  $\hbar\omega(x)-E^{up}>0$ ], the temperature increases as the transmission decreases (see Fig. 4). The shift of the excitonic part of the polariton and low transmission extend to large negative detuning and allow efficient heating. If one starts from negative values for the detuning, the sample is cold even beyond the ‘‘cutoff’’ ( $\zeta$ ) energy. Transmission remains close to unity, and photothermal heating is inefficient. This means that the equilibrium states for the cold (up-going) scan and already heated (down-going) scan are different. Let us consider the down-going scan. When one moves up to the polariton upper branch energy, the transmission decreases—which increases the sample temperature. At some point (cutoff energy), the heating becomes dominant over the cooling, and we face a

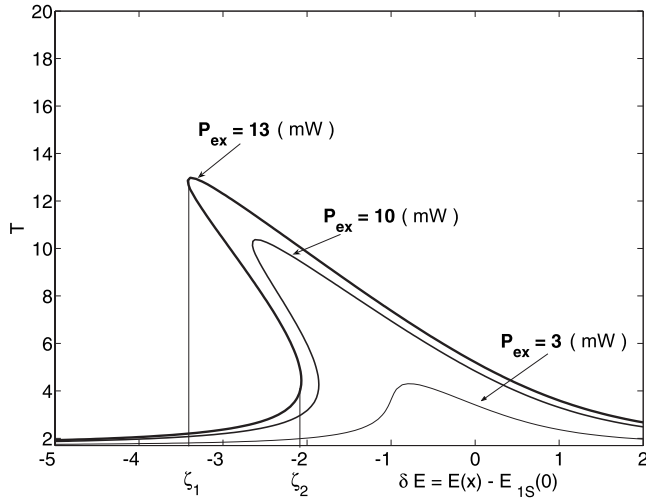


FIG. 4. The first equation of the system (7) is visualized as an implicit function of the local sample temperature  $T$  and detuning  $\delta E$  from the resonance energy for different excitation intensities  $P_{ex}$ . The redshift of the maximum is accompanied by the bistability effect.

rapid temperature drop. The range of this bistability mainly depends on laser pulse intensity  $P_{ex}$ .

For a quantitative numerical calculation of the resulting dispersion curves, one has to resolve the nonlinear system of equations (4) and (7) at equilibrium using standard perturbation theory. As a result of the nonlinear origin of the temperature equation, there are four different polariton branches corresponding to the up- and down-scan (see Fig. 5), on which the bistability effect manifests itself as an abrupt drop in the temperature from red color of large temperature to blue color of cold helium.

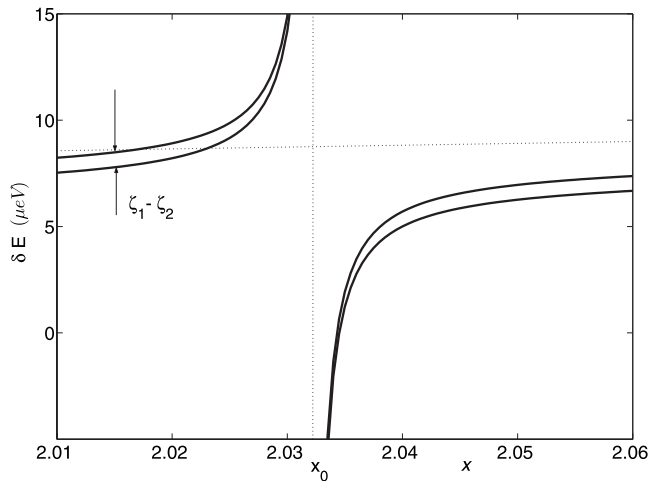


FIG. 5. The resulting branches of the quadrupole-LA phonoriton dispersion are represented by the solid lines. The dashed lines correspond to noninteracting photon (vertical) and 1S quadrupole exciton (horizontal). The laser intensity is taken to be  $P_{ex} = 5$  mW. The bistability range for the excitonlike part of the phonoriton is  $\zeta_1 - \zeta_2 \approx 2$   $\mu\text{eV}$ . Actual population of the branches depends on the initial condition and up- or down-going scan. Also, in the case of high light intensity  $P_{ex} > 57$  mW, interconversion processes can occur due to optical  $\Gamma_{12}^-$  phonons.

## V. RESULTS AND DISCUSSION

The most important result which emerges from the dispersion curves in the case of pumping by short pulses is the existence of a *localized state* on the lower branch of the polariton (Fig. 3). So on a microsecond time interval, one can observe replicas of these states in the luminescence spectra due to intense polariton buildup in this state.

Let us compare the polariton “bottleneck” first proposed by Toyozawa<sup>21</sup> and the polariton density buildup at the localized state we proposed. The bottleneck is a consequence of the sharp drop in the density of states at the knee of the lower polariton branch. This results in a lifetime of the polariton having a peak at that region. For the conventional dipole-allowed polariton, the lifetime is not long enough for the thermalization of the polariton. However, the quadrupole-allowed exciton has less pronounced interaction with photon and, therefore, the drop in the density of state allows polariton thermalization with acoustical phonon bath. As a consequence, the polariton dispersion is weakly perturbed and shows an unstable maximum at the lower polariton branch knee. At that maximum, the polariton density buildup occurs due to small group velocity and big density of states. That is, the bottleneck is a necessary condition for the density buildup, but this two phenomena have absolutely different origins.

The evidence of such a build-up of polariton density can be demonstrated in the collapse and revival of the quantum beats of the scattered probe signal.<sup>22</sup> The luminescence from this highly unstable state can be considered as a signature of the polariton perturbation by the LA phonons and can be utilized to produce delayed laser pulses. The states on the upper branch have bigger group velocity compared to standard polariton modes, and this can effectively prevent BEC as the polaritons escape the crystal more effectively.

In the case of long pump pulses, an even more effective mechanism which prevents BEC is provided by the bistability effect. Indeed, it was demonstrated by Ell *et al.*<sup>3</sup> that the BEC for excitation of states with sufficiently low oscillator strength is possible only when the kinetic energy of the excitonic part of the pump polariton is bigger than the splitting between the polariton branches at resonance. The latter prevents the polariton from “condensing” outside of the crystal. This condition certainly fails for the cuprous OE polaritons, since the kinetic energy is about 9  $\mu\text{eV}$  and the Rabi splitting is 127  $\mu\text{eV}$ . Moreover, the adiabat (4) never crosses the condensation line  $T_c = n_0^{2/3} \times 10^{-11}$ .

However, PEs in cuprous oxide are good candidates for possible BEC and live long enough ( $> 10$  ms) to reach equilibrium because the Rabi splitting is  $\hbar\Omega_p = \hbar\Omega_o \sqrt{f_p/f_o} = 1.1$   $\mu\text{eV}$  for 1 T magnetic field,<sup>23</sup> which is eight times less than the kinetic energy. For rather large intensity of the pumping laser, according to the results of our work, the polaritons are perturbed by the weak interaction with LA phonons. Hence, due to the long lifetime of the para-exciton, one has a splitting of the upper and lower polariton branches into four other ones due to bistability. The extremely small oscillator strength for this para-exciton transition  $f_p = 4f_o \times 10^{-3}$  supports the condensation condition stated above for films starting from  $d_s > 0.7$  mm thickness.<sup>24</sup>

The upper and lower PE polariton branches are also split into four new ones due to bistability effect, in close analogy to the OE polariton. Let us estimate the effective splitting between all pairs of polariton branches. According to the second equation of the system (4), to reach the critical condensation density of  $n_c \approx (9T_{bath} \times 10^{11})^{3/2} = 1.89 \times 10^{18} \text{ cm}^{-3}$  at the point of resonance with light, one needs the intensity of the laser field to be  $P_{ex} = 185 \text{ mW}$ . In this case, the calculated region of bistability is about  $\zeta_1 - \zeta_2 = 25 \text{ } \mu\text{eV}$ , which is approximately two times bigger than the kinetic energy of the PE. As a result, BEC of the PE polaritons may be effectively *suppressed* by the bistability effect.

In conclusion, we would like to briefly outline possible deviations from the linear model of the temperature dependent exciton energy in cuprous oxide crystals which we used. If one has to consider the influence of the bistability effect on the possible BEC of the polariton or for high intensity of the pumping laser  $P_{ex} > 35 \text{ mW}$  when the temperature increase is bigger than 87 K, then the linear approximation for the temperature dependence of the gap energy given by Eq. (4) may not be applicable.

Therefore, one has to apply a more elaborate expression for the exciton energy  $E_{1S}(T, x) \rightarrow E_{1S}(T, x, \rho)$  including a contribution from the optical phonons.<sup>10,18</sup> The parameter  $\rho$  controls the relative contribution of the long-wavelength acoustic phonons  $\rho \rightarrow 1$ , on one hand, and those of optical and short-wavelength acoustical phonons, on the other hand,  $\rho \rightarrow 0$ . The dielectric background constant  $\epsilon_\infty$  becomes a linear function of the wave vector.

Due to the complexity of the full expression, it is useful to consider some approximations. When the acoustic phonons dominate, this expression transforms into the familiar Bose-Einstein model proposed by Weiser:<sup>25</sup>

$$\hbar\omega_{1S}(T) = \hbar\omega_{1S}(0) - a \left[ 1 + \frac{2}{\exp(\Theta/T) - 1} \right].$$

Here, there are two fitting parameters  $a$  and  $\Theta$ . Both emission and absorption of phonons are now considered. For the LA phonons, the main contribution to the exciton energy can be fitted with the empirical relation proposed by Varshi:<sup>26</sup>

$$\hbar\omega_{1S}(T) = \hbar\omega_{1S}(0) - \frac{\alpha T^2}{T + \Theta}.$$

Experiment<sup>11</sup> shows that for the bulk cuprous oxide,  $\alpha = 4.8 \times 10^{-7} \text{ eV/K}$ .

## ACKNOWLEDGMENTS

We would like to acknowledge Upali Aparajita for useful comments and discussion on the manuscript. This project was supported in part by PCS-CUNY.

## APPENDIX

The comprehensive review paper of Fernandez-Rossier *et al.*<sup>27</sup> deals with exciton high density effects as the density approaches saturation. Here, we apply their theory to bulk cuprous oxide. The 1S exciton energy experiences a blueshift due to exchange interaction between electrons and holes, and redshift due to increased screening:

$$\Delta E^{blue} = \frac{13\pi}{3} \hbar\omega_{1S,0} n a_B^3,$$

$$\Delta E^{red} = f_o(\omega) \hbar\omega_{1S,0} \pi n a_B^3.$$

The screening spectral function is given by the following expression:

$$f(\varpi) = \frac{\varpi(32 + 63\varpi + 44\varpi^2 + 11\varpi^3)}{(1 + \varpi)^4} - \frac{8\varpi(4 + 3\varpi)}{(1 + \varpi)^2}$$

and  $\varpi^2 = (1 + m_h/m_e)^2 / (4m_h/m_e)$ . These effects partially compensate each other.

To estimate the net shift, let us take, for example, the following numerical values:  $P_{ext} = 5 \text{ mW}$  is the laser field intensity,  $d = 1 \times 10^{-6} \text{ m}$  is the diameter of the focused laser beam,  $v_g = 4 \times 10^4 \text{ m/s}$  represents the group velocity of the pump polariton, and the factor 4 indicates the fact that we excite both OE and PE;  $m_e = 0.69m_0$  and  $m_h = 0.99m_0$  are the effective mass for electron and hole.

Due to the small quadrupole exciton radius, the net shift:  $\Delta E^{red} - \Delta E^{blue} = -0.226 \text{ } \mu\text{eV}$ . Hence, it is much less compared to the redshift due to the heating:  $-2.1 \text{ } \mu\text{eV}$ . However, the situation will change drastically for a two-dimensional quantum well, as in this case the blueshift dominates due to exchange energy. Note that these estimations are valid for any duration of the pulses required to build up the necessary polariton density.

The oscillator strength is proportional to the gap energy of cuprous oxide,<sup>28</sup> and so depends on the temperature also. It gets smaller with the increase of the pumping power. The relative change of the oscillator strength is  $\approx 1.4 \times 10^{-3}$  for  $T - T_{bath} = 20 \text{ K}$ , but because it is not a resonant term, we neglect this effect. For the same reason, we neglect the temperature dependence of the linewidth.<sup>11</sup>

<sup>1</sup>D. W. Snoke, A. J. Shields, and M. Cardona, Phys. Rev. B **45**, 11693 (1992).

<sup>2</sup>D. Fröhlich, G. Dasbach, H. Baldassarri Höger, M. Bayer, R. Klieber, D. Suter, and H. Stolz, Solid State Commun. **134**, 139 (2005).

<sup>3</sup>C. Ell, A. L. Ivanov, and H. Haug, Phys. Rev. B **57**, 9663 (1998).

<sup>4</sup>D. W. Snoke and S. A. Moskalenko, *Bose-Einstein Condensation of Excitons and Biexcitons: And Coherent Nonlinear Optics with Excitons* (Cambridge University Press, Cambridge, England, 2000).

<sup>5</sup>M. Inguscio, S. Stringari, and C. Wieman, *Bose-Einstein Condensation in Atomic Gases: Course CXL: Varenna on Lake Como*

- Villa Monestero, 07-17 July 1998* (IOS, Amsterdam, 1999).
- <sup>6</sup>D. W. Snoke, J. P. Wolfe, and A. Mysyrowicz, *Phys. Rev. Lett.* **64**, 2543 (1990).
- <sup>7</sup>G. M. Kavoulakis, G. Baym, and J. P. Wolfe, *Phys. Rev. B* **53**, 7227 (1996).
- <sup>8</sup>I.e., they exhibit a “quantum saturation.”
- <sup>9</sup>The temperature is low enough to neglect contributions from the optical phonons.
- <sup>10</sup>A. Mysyrowicz, D. Hulin, and A. Antonetti, *Phys. Rev. Lett.* **43**, 1123 (1979).
- <sup>11</sup>G. Dasbach, G. Baldassarri Hoger von Hogersthal, D. Fröhlich, H. Stolz, and M. Bayer, *Phys. Rev. B* **70**, 121202(R) (2004).
- <sup>12</sup>B. S. Wang and J. L. Birman, *Phys. Rev. B* **42**, 9609 (1990).
- <sup>13</sup>L. Hanke, D. Fröhlich, A. L. Ivanov, P. B. Littlewood, and H. Stolz, *Phys. Rev. Lett.* **83**, 4365 (1999).
- <sup>14</sup>A. L. Ivanov and L. V. Keldysh, *Zh. Eksp. Teor. Fiz.* **84**, 404 (1982).
- <sup>15</sup>L. Keldysh and S. Tikhodeev, *Zh. Eksp. Teor. Fiz.* **63**, 1086 (1986).
- <sup>16</sup>Polariton  $\rightarrow$  phonon bath.
- <sup>17</sup>Phonon bath  $\rightarrow$  polariton.
- <sup>18</sup>R. Passler, *J. Appl. Phys.* **83**, 3356 (1998).
- <sup>19</sup>For the OE, it comes close to the condensation line  $n_0 \propto T^{3/2}$  at high density of the exciton gas, but never crosses. For the PE, there is BEC critical temperature given by the cross point.
- <sup>20</sup>As an alternative to iterations, one can approach the desirable intensity by changing it gradually.
- <sup>21</sup>Y. Toyozawa, *Optical Processes in Solids* (Cambridge University Press, Cambridge, England, 2003).
- <sup>22</sup>D. Fröhlich, A. Kulik, B. Uebbing, A. Mysyrowicz, V. Langer, H. Stolz, and W. von der Osten, *Phys. Rev. Lett.* **67**, 2343 (1991).
- <sup>23</sup>The para-excitons are optically inactive without external perturbation. We took the magnetic field perturbation just as an example so that the para-excitons gain some oscillator strength.
- <sup>24</sup>K. Kapinska, P. Loosdrehta, I. Handayania, and A. Revcolevschi, *J. Lumin.* **112**, 17 (2005).
- <sup>25</sup>G. Weiser, *Phys. Rev. B* **45**, 14076 (1992).
- <sup>26</sup>Y. Varshi, *Physica (Amsterdam)* **34**, 149 (1967).
- <sup>27</sup>J. Fernandez-Rossier, C. Tejedor, L. Munoz, and L. Vina, arXiv:cond-mat/9510138 (unpublished).
- <sup>28</sup>S. A. Moskalenko and M. A. Liberman, *Phys. Rev. B* **65**, 064303 (2002).